coatings

MDPI

Article

Effect of Surface Modification of PEEK Artificial Phalanx by 3D Printing on its Biological Activity

Yun Shi †, Ting Deng †, Yu Peng, Zugan Qin, Murugan Ramalingam, Yang Pan, Cheng Chen, Feng Zhao, Lijia Cheng * and Juan Liu *

School of Basic Medical Sciences, Institute for Advanced Study, Mechanical Engineering College, Chengdu University, Chengdu 610106, China

* Correspondence: chenglijia@cdu.edu.cn (L.C.); liujuan@cdu.edu.cn (J.L.)

† These authors contributed equally to this work.

Abstract: Objective: Polyetheretherketone (PEEK) is widely used as an orthopedic implant material owing to its good biocompatibility and mechanical strength; however, PEEK implants are biologically inert, resulting in suboptimal cellular responses after implantation. The aim of this study was to enhance the biological activity of PEEK through sulfonation treatment. Methods: In this study, distal phalangeal implants of PEEK were customized by fused deposition modeling (FDM) printing technology and soaked in concentrated sulfuric acid at different times to obtain sulfonated PEEK (SPEEK). The groups were divided into five groups according to the sulfonation time as follows: 0 min (control group), 1 min (group SPEEK1), 2 min (group SPEEK2), 4 min (group SPEEK4), and 8 min (group SPEEK8). Then the physicochemical characteristics of implants were determined by SEM, XRD, EDS, etc. The implants were co-cultured with stem cells from human exfoliated deciduous teeth (SHED), and then the cell proliferation, adhesion, alkaline phosphatase (ALP) activity, and alizarin red staining were performed to detect the biological activity, biocompatibility, and osteogenic activity of the SPEEK implants. Results: The sulfonation time range of 1 to 8 min could promote the formation of micropores on the surface of PEEK implants, while slightly affecting the composition and compression performance of the implants. Compared with the control group, the hydrophilicity of PEEK materials was not improved after sulfonation treatment. Tests for adhesion and proliferation of SHED indicated that SPEEK2 showed superior biocompatibility. Furthermore, ALP activity and semi-quantitative analysis of Alizarin red staining showed that the osteogenic activity of SPEEK2 phalanges exhibited significantly stronger osteogenic activity than the other groups. Conclusions: The method presented here provides a promising approach to improve the surface bioactivity of PEEK implants prepared by FDM, providing a shred of primary evidence to support the application of SPEEK in orthopedics.

Keywords: polyetheretherketone; FDM; surface modification; sulfonation; bioactivity

Citation: Shi, Y.; Deng, T.; Peng, Y.; Qin, Z.; Ramalingam, M.; Pan, Y.; Chen, C.; Zhao, F.; Cheng, L.; Liu, J. Effect of Surface Modification of PEEK Artificial Phalanx by 3D Printing on its Biological Activity. *Coatings* **2023**, *13*, 400. https://doi.org/10.3390/coatings13020400

Academic Editor: Catalina Natalia Cheaburu-Yilmaz

Received: 13 January 2023
Revised: 2 February 2023
Accepted: 8 February 2023
Published: 9 February 2023

1. Introduction

Clinically, most of the metacarpophalangeal joints require direct amputation after severe injury [1]. In recent years, polyetheretherketone (PEEK) has attracted extensive attention as a promising biomaterial candidate for orthopedic substitutes due to its excellent mechanical properties, biocompatibility, high-temperature durability, chemical stability, and radiolucency, especially in similar elastic modulus to cortical bone [2–4]. As 3D printing technology continues to mature, more and more researchers and surgeons are using it to fabricate implants. Due to its unique advantages, 3D printing technology is combined with CT, MRI, and other medical scanning technologies to customize implants of PEEK [5,6]. However, PEEK substitutes are relatively hydrophobic and biologically inert, which caused unsatisfactory and poor integration with surrounding tissues that hampers its long-term clinical success when they were implanted into the patients [7].

Therefore, improving the bioactivity of PEEK is a major challenge that must be addressed to fully realize its potential benefits. Currently, the bioactivity of most PEEK implants is improved by blending with bioactive materials. For example, bioactive particles such as carbon fiber (CF), hydroxyapatite (HA), nano-titanium dioxide (n-TiO_2), and calcium silicate (CS) powders were blended into PEEK scaffolds to improve the bioactivity and osseointegration greatly [8–13]. Lu et al. utilized plasma immersion ion implantation (PIII) to integrate Ta_2O_5 nanoparticles onto a PEEK surface for improving the proliferation and osteogenic differentiation of rat bone mesenchymal stem cells (rBMSCs) for potential osteointegration [14]. However, because of the weak connection between PEEK and the bioactive particles, the composite method added a second phase to the bulk PEEK matrix, which could lead to long-term mechanical and stability difficulties [15]. It is also a challenge to improve the bioactivity of PEEK materials without affecting their physical properties.

In addition to the above strategies that blend PEEK with bioactive materials, another interesting strategy of surface modification is to establish a microporous structure on solid PEEK surface. Dos Santos et al. treated a PEEK surface with piranha solution to promote bioactivation of the PEEK surface [16]. In this study, we focused on sulfonation treatment, which was also considered to be an effective approach to improve osseointegration of the bone–PEEK interface [17–19]. Sulfonation can not only introduce charged sulfonate (-SO_3-) groups into the main chain of the polymerization to increase the hydrophilicity of PEEK, but also the sulfonic polymer scaffold can increase the non-specific interaction between the scaffold and glycocalyx molecules on the outer membrane of the cell, thus enhancing the proliferation and adhesion of osteoblasts [20–24]. Wan et al. employed gaseous sulfur trioxide (SO_3) to fabricate a porous surface of PEEK implants for various times, which significantly enhanced the cytocompatibility and bioactivity of PEEK implants [25].

In this study, we combined a fused deposition modeling (FDM) and sulfonation process to produce the distal phalanx of the index finger with microporous structure for enhancing bioactivity and osseointegration. The influence of sulfonation in different reaction times on the micropore uniformity and compression performance of the distal phalanx of index finger prepared by FDM were investigated through SEM and compression test. Cell culture experiments were further conducted to evaluate the effect of the treatment on the biological properties of the modified PEEK surface through CCK-8, ALP activity, Alizarin red staining, etc.

2. Materials and Methods

2.1. Material Preparation

2.1.1. Raw Materials

Biomedical-grade PEEK filament with a diameter of 1.75 mm was obtained from Victrex Manufacturing Ltd. (Lancashire, UK) for FDM. Sulfuric acid (95–98 wt.%) and acetone (>99 wt.%) were purchased from Sinopharm Chemical Reagent Co. Ltd. (Shanghai, China).

2.1.2. FDM-Fabricated PEEK Distal Phalanx

The distal phalanx of the index finger structures was fabricated by a FDM system (Sandi Tribal Technology Co., Ltd., Shanghai, China). Briefly, the data of the hand were obtained by high-resolution helical CT (Amsterdam, Philips, The Netherlands) scanning and imported into Materialise Mimics21.0 (Materialise, Leuven, Belgium) to generate point cloud data, which were then imported into engineering design software NX 12.0 (Siemens, Munich, Germany) to design and save in STL format. Finally, the data were imported into Simplify 3D software (Cincinnati, OH, USA) for slicing and then loaded into the FDM system. The printing parameters of FFF, namely the printing speed, nozzle temperature, nozzle diameter, and layer thickness, were fixed at 20 mm/s, 380 °C, 0.4 mm, and 0.2 mm, respectively.

2.1.3. Sulfonation Treatment of PEEK Implants

The sulfonation treatment process was performed by fully immersing the FDM-printed PEEK structures into high-concentration sulfuric acid according to previous methods [26,27]. Briefly, all PEEK samples were cleaned by ultrasonic washing (DM6-E200A, China) with acetone, ethanol, and ultrapure water for 10 min, respectively. Then the samples were immersed into concentrated sulfuric acid for 1 min (SPEEK1), 2 min (SPEEK2), 4 min (SPEEK4), and 8 min (SPEEK8) at room temperature, during which they were stirred continuously with a magnetic stirrer (WH220-HT, WIGGENS, Straubenhardt, Germany). At the end of the sulfonic reaction of each sample, ultrasonic cleaning with acetone, ethanol, and ultrapure water was performed for 10 min successively, and finally autoclave steam sterilization was performed for 1 h to remove the residual concentrated sulfuric acid on the surface of the sample. The untreated PEEK after the same clean and sterilization as the SPEEKs was used as the control. Next, all samples were ultrasonic cleaning for 10 min and autoclave steam sterilization for 1 h before experiments.

2.2. Physical–Chemical Characteristics of SPEEKs

2.2.1. Surface Morphology and Chemical Composition

The surface topography and chemical composition of the prepared samples were characterized by high-resolution electron microscope (HREM, JIB-4700F, JEOL, Tokyo, Japan) and X-ray diffractometer (XRD, D8 ADVANCE, Bruker, Karlsruhe, Germany). The purpose of the HREM is to observe the atomic arrangement image of the material formed by the phase difference between the synthesized projected wave and the diffracted wave. The materials were treated with gold spraying before HREM observation. The principle is to spray gold powder on the surface of the material; under the electrostatic action, gold will be uniformly adsorbed on the surface of the workpiece, forming a coating. The coating is cured by baking at a high temperature and becomes the final coating with different effects. After surface spraying, the mechanical strength, adhesion, corrosion resistance, and aging resistance of the material can be significantly improved. Then the materials were observed at magnifications of 2000×, 4000×, and 10,000×, and the elements of the materials were determined by the energy disperse spectroscopy (EDS) under HREM. Next, the XRD uses the diffraction principle to accurately determine the texture of the material. Then the characteristic peaks were analyzed based on the diffraction data.

2.2.2. Surface Roughness

Three samples were selected from each group, cleaned three times by sonication with deionized water, and then dried overnight at 37 °C. Using SuperView W1 profilometer (Shenzhen, China), five points on each sample surface were selected for determination, and the average value was taken as the sample roughness, Ra.

2.2.3. Hydrophilic Properties

We analyzed the material's hydrophilic properties by measuring the contact angle, i.e., the angle between the tangential line of the gas–liquid interface and the solid–liquid boundary at the intersection point of gas, liquid, and solid. In order to determine the hydrophilic properties of the surface of the material, we used the contact angle tester (SL200B, Shanghai, China) to gauge the water contact angle, which was measured by the sessile drop method [28]. Firstly, six samples were selected from each group; we washing them with deionized water three times and then dried them overnight at room temperature. Secondly, five measurements were carried out at different positions on the surface of each sample. Lastly, the water contact angle was calculated through measuring the average angle on both sides of the droplet with built-in software. The main process of calculation is grayscale, binarization, and denoising to complete the initial image processing.

2.2.4. Mechanical Testing

Three samples were selected for each group, and the samples were ultrasonically cleaned with deionized water three times and dried overnight at 37 °C. A microcomputer-controlled electronic universal experimental machine (WDW-50D, Jinan, China) was used for the compression test. To carry out the compression test smoothly, the sample shaped at the end of the finger was ground into a flat structure before the test. During the compression test, the polished sample was placed vertically on the test table, and the descent speed of the universal testing machine was controlled to compress the sample downward at a slow and uniform speed until the sample was compressed and fractured. The sample shape was in accordance with the GB/T1041-2008 standard. The sample were placed horizontally, and the strain rate was adjusted to 1.4×10^{-4} s^{-1} at room temperature. The compressive stress–strain curve was obtained by taking the average value after three tests.

2.3. Biocompatibility and Osteogenic Ability of SPEEKs

2.3.1. Cell Separation and Culture

Stem cells from human exfoliated deciduous teeth (SHED) used in this study were routinely cultured. The collected deciduous teeth were placed in an ultra-clean table after disinfection with ultraviolet light. The deciduous teeth were repeatedly rinsed with PBS solution, and the pulp tissue was extracted by a pulp-extraction needle and was put into an EP tube containing a-MEM medium and cut into pieces. The pulp tissues were collected by mixed digestion with collagenase type I and dispase in a 1:1 ratio and then left in a water bath at 37 °C for 1 h. After centrifugation at 1000 r/min for 5 min, the supernatant was discarded, and the culture medium was added to mix and blow. The cell suspension obtained by filter mesh was inoculated into the culture flask, and an appropriate amount of a-MEM medium containing double antibody and 20% FBS was added and then cultured in an incubator, at 37 °C, with 5% CO_2. After the cells were fused into monolayers, they were digested by using 0.25% trypsin for 3 min at room temperature. After centrifugation at 1000 r/min for 5 min; the supernatant was discarded; and the precipitate was blown, mixed, and passaged at a ratio of 1:3.

2.3.2. Cell Adhesion and Proliferation

In order to observe the adhesion and proliferation of cells, the adhesion ability of cells was evaluated by observing the number of cells on the surface of the material. SHED was seeded on the samples in a 24-well plate at a density of 2×10^4 cells per well and cultured for 1, 4, and 7 days at 37 °C, 5% CO_2. Afterward, samples with cells were washed twice with PBS and fixed in 4% formaldehyde for 15 min. The nuclei of SHED were stained with 40, 60-diamidino-2-phenylindole (DAPI, Solarbio Science & Technology Co., Ltd., Beijing, China) for 5 min and observed under fluorescence microscope.

The Cell Counting KIT-8 (CCK-8, Dojindo Laboratories Inc., Kumamoto, Japan) assay was used to evaluate the viabilities of SHED on different samples. Optical density (OD) was determined using a spectrophotometer (Bio-Tek, Winooski, VT, USA) at a wavelength of 450 nm.

2.3.3. Biocompatibility of SPEEKs

Scanning electron microscopy (SEM, JIB-4700F, JEOL, Tokyo, Japan) was used to observe the spreading morphology and state of cells on the surface of the materials. SHED was seeded in 24-well plates at a density of 2×10^4 cells per well and cultured for 24 h. All materials were first washed with PBS to remove non-adherent cells, and after being fixed with paraformaldehyde for 15 min, they were washed twice with PBS. The samples were dehydrated by a gradient with different concentrations of ethanol (30%, 50%, 70%, 80%, 90%, 95%, and 100% v/v) for 30 min each [15]. The morphology of adherent cells was observed by SEM after spraying gold.

2.3.4. The Osteogenic Potential of SHED Induced by SPEEKs

SHED was implanted into samples at a density of 2×10^4 cells per well in 24-well plates and incubated for 7, 14, and 21 days. After 7 and 14 days of culture, alkaline phosphatase staining was performed according to the manufacturer's instructions. Semi-quantitative analysis of ALP activity was performed using the ALP detection kit (Beyotime, Shanghai, China), according to the method specified in the user manual. After 21 days of the induction period, calcium nodule formation (mineralization) was analyzed by Alizarin red staining (ARS), and semi-quantitative Alizarin red analysis was performed.

2.4. Statistical Analysis

All experimental data were statistically analyzed by statistical software IBM SPSS 20.0 (Armonk, New York, NY, USA). The data of surface roughness, water contact angles, cell growth, cell viability, ALP activity, and semi-quantitative analysis of Alizarin red staining between groups were expressed as mean ± SD and compared by using a t-test and one-way analysis of variance for statistical analysis. Statistical significance was set at $p < 0.05$.

3. Results

3.1. Surface Morphology and Chemical Characterization of SPEEKs

The surface morphology of the PEEK material was relatively smooth, with some protrudes and gullies, which might be caused by poor 3D-printing-process parameters (Figure 1a). When the sulfonation treatment time was 1 min, some relatively uniform microporous structures began to appear on the surface of SPEEK1, with an average microporous diameter of (0.61 ± 0.18) μm (Figure 1b). As the time increased from 1 to 2 min, a highly uniform and complex microporous structure was generated on the entire SPEEK2 surface, with an average microporous diameter of (0.71 ± 0.11) μm (Figure 1c). Compared to SPEEK1, the pore size of SPEEK2 increased slightly, and the porosity increased significantly. As the time increased to 4 min, the average pore diameter of the highly interconnected micropore structure was increased significantly to (0.91 ± 0.25) μm, which gradually approximated a circle (Figure 1d). However, when the time was further increased to 8 min, it was observed that the porous structures formed on the surface layer of the material were disrupted and dissolved, which may be caused by the excessive soaking time (Figure 1e).

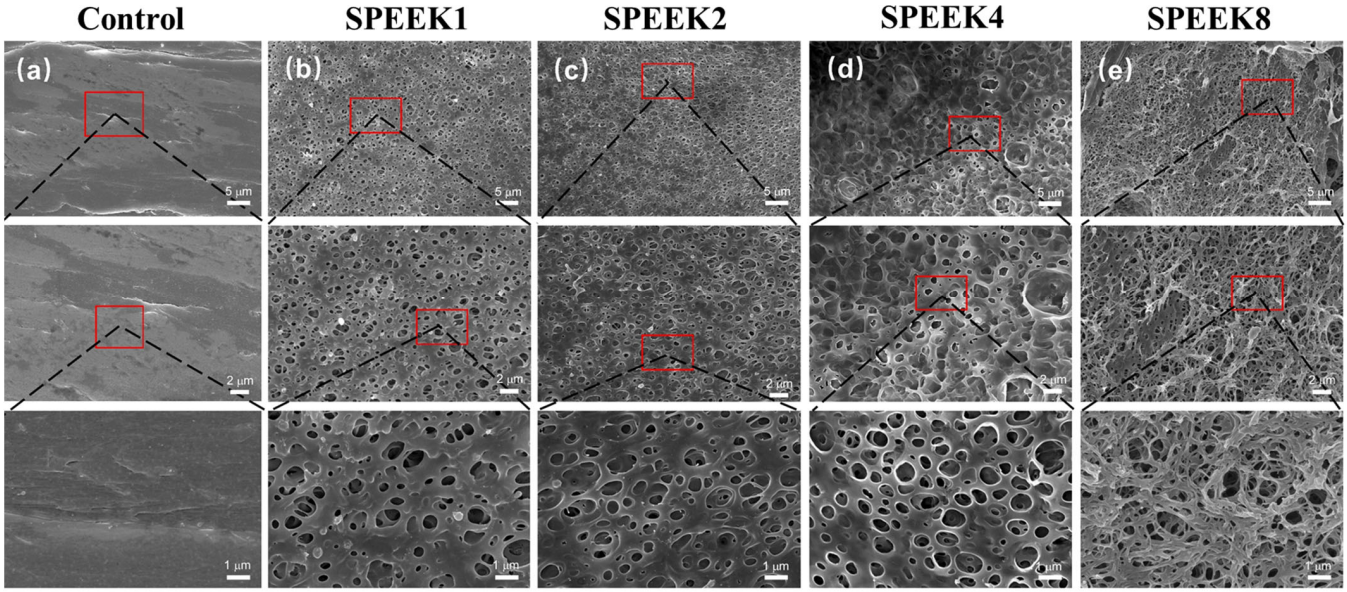

Figure 1. SEM images of FDM-printed PEEK and SPEEK index finger with sulfonation treatment of (**a**) 0 min (Control), (**b**) 1 min (SPEEK1), (**c**) 2 min (SPEEK2), (**d**) 4 min (SPEEK4), and (**e**) 8 min (SPEEK8), respectively. From top to bottom, magnifications of 2000×, 4000×, and 10,000× were used.

The energy-dispersive spectrometer (EDS) analysis showed that C, O, and S elements were present on the PEEK materials, indicating that the S element was introduced into the 3D porous network structure through sulfonation. When the PEEK index finger was treated, the sulfonic acid (-SO_3H) group was introduced into the ortho position of the hydroquinone segment on the PEEK surface by direct electrophilic substitution reaction [29,30]. It resulted in the sulfur element in the EDS spectra of the treated SPEEK samples, and the S concentration showed an increasing trend with time. The S concentration of SPEEK4 was significantly higher than that of other SPEEK groups (Figure 2a,b).

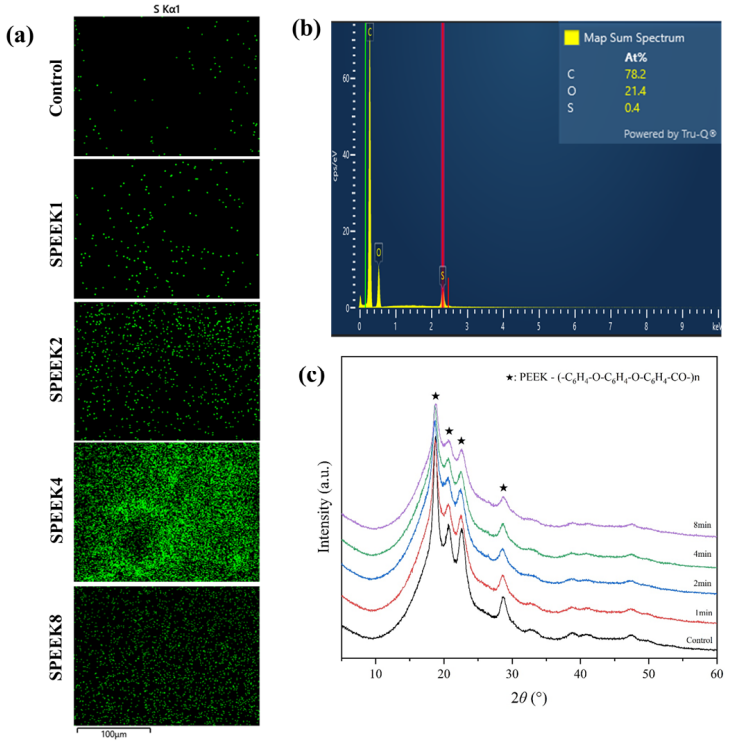

Figure 2. (**a**) The S element distribution of 3D-printed PEEK index finger under different sulfonation treatment times by EDS. Scalebar: 100 μm. (**b**) The elemental composition spectrum of SPEEK4 after sulfonation treatment for 4 min. (**c**) The XRD patterns show the composition of PEEK materials before and after sulfonation treatment.

It can be seen from the XRD patterns that there was no significant difference between PEEK samples before and after surface modification, and all of them had four obvious characteristic peaks, 2θ, being 18.7°, 20.7°, 22.5°, and 28.6° (Figure 2c). This indicates that, for PEEK, after sulfonation modification, the introduced sulfonic acid group cannot destroy the structure of the material, the crystallization performance is not changed, and it still has good crystallization performance.

The surface roughness of the sample was examined by using profilometry (Figure 3a), and the data after the examination were analyzed (Figure 3b). Compared with the control group, the surface roughness of the SPEEKs increased significantly with the increase in the sulfonation time. As shown in Figure 3b, the surface roughness of SPEEKs was considerably higher than that in the control group [Ra = (0.22 ± 0.02) μm]. Moreover, when the PEEK surface is transformed from a smooth surface without any treatment to an etched pore structure and a three-dimensional mesh-like pore structure, the surface roughness increases significantly. Still, the surface roughness will decrease if the pore structure collapses. When sulfonated for 1 min, the surface roughness, Ra, of the PEEK sample increased from (0.22 ± 0.02) μm to (4.37 ± 0.26) μm. With the sulfonation time up to 2 min, the surface roughness of the sample reached the maximum [Ra = (5.19 ± 0.22) μm]. When the sulfonation time was 4 min, the surface roughness of SPEEK4 began to

decrease [Ra = (2.07 ± 0.13 μm], indicating that the pore structure on the surface of the PEEK sample began to collapse at this time. As the sulfonation treatment continued for 8 min, the surface roughness of the PEEK increased again [Ra = (2.73 ± 0.17) μm], which was due to the large area of the collapse of the surface network structure of the sample caused by excessive dissolution. These results showed that the sulfonation treatment can effectively improve the surface roughness of the PEEK distal phalanx, and the sulfonation time of 2 min was the most suitable.

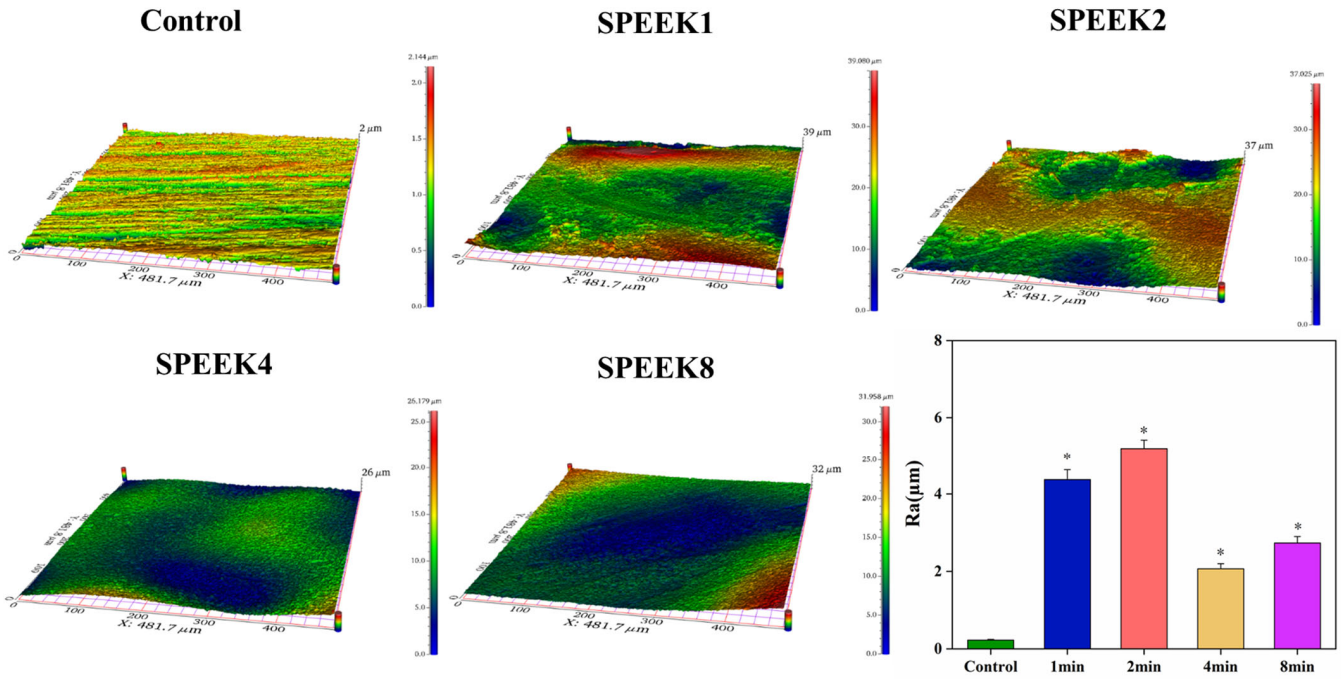

Figure 3. The 3D image of the material surfaces and their statistical analysis of material surface roughness (n = 5, * $p < 0.05$ vs. control group).

3.2. Hydrophilic Properties of SPEEKs

The contact angle of biomaterials is an important indicator that reflects their hydrophilicity, which directly affects the degree of wear of the material surface in the human body. Additionally, the hydrophilicity not only can affect the ability of the implant materials to adhere to proteins and cells in the tissue, but directly promotes the differentiation of osteocytes and the proliferation of osteoblasts. Although PEEK contains a large number of polar hydrophilic groups, ether bonds, and ketone groups, its long molecular chain contains a large number of benzene rings, making it a hydrophobic material. Previous studies have shown that changes in surface morphology and the introduction of sulfonic acid groups can have varying degrees of effect on the hydrophilicity of the PEEK surface. In our study, the contact angles of PEEK and SPEEK corresponding to four groups were measured, and their contact-angle profiles are shown in Figure 4a.

After being modified with concentrated sulfuric acid, the water contact angles of PEEK changed from 65.21° ± 1.81° to 75.13° ± 2.06° for SPEEK1, 70.24° ± 2.50° for SPEEK2, 74.46° ± 2.11° for SPEEK4, and 79.67° ± 2.27° for SPEEK8. It can be found that the contact angle of each SPEEK group was higher than that of the PEEK group, but there was no significant difference between the different SPEEK groups (Figure 4b). The previous results also found that the water contact angle of the material surface increased and the hydrophilicity decreased after sulfonation treatment; such findings are consistent with the present results. This indicates that the surface hydrophilicity of PEEK materials was not improved after sulfonation treatment, and there was no obvious correlation between the hydrophilicity of SPEEKs with different sulfonation treatment times.

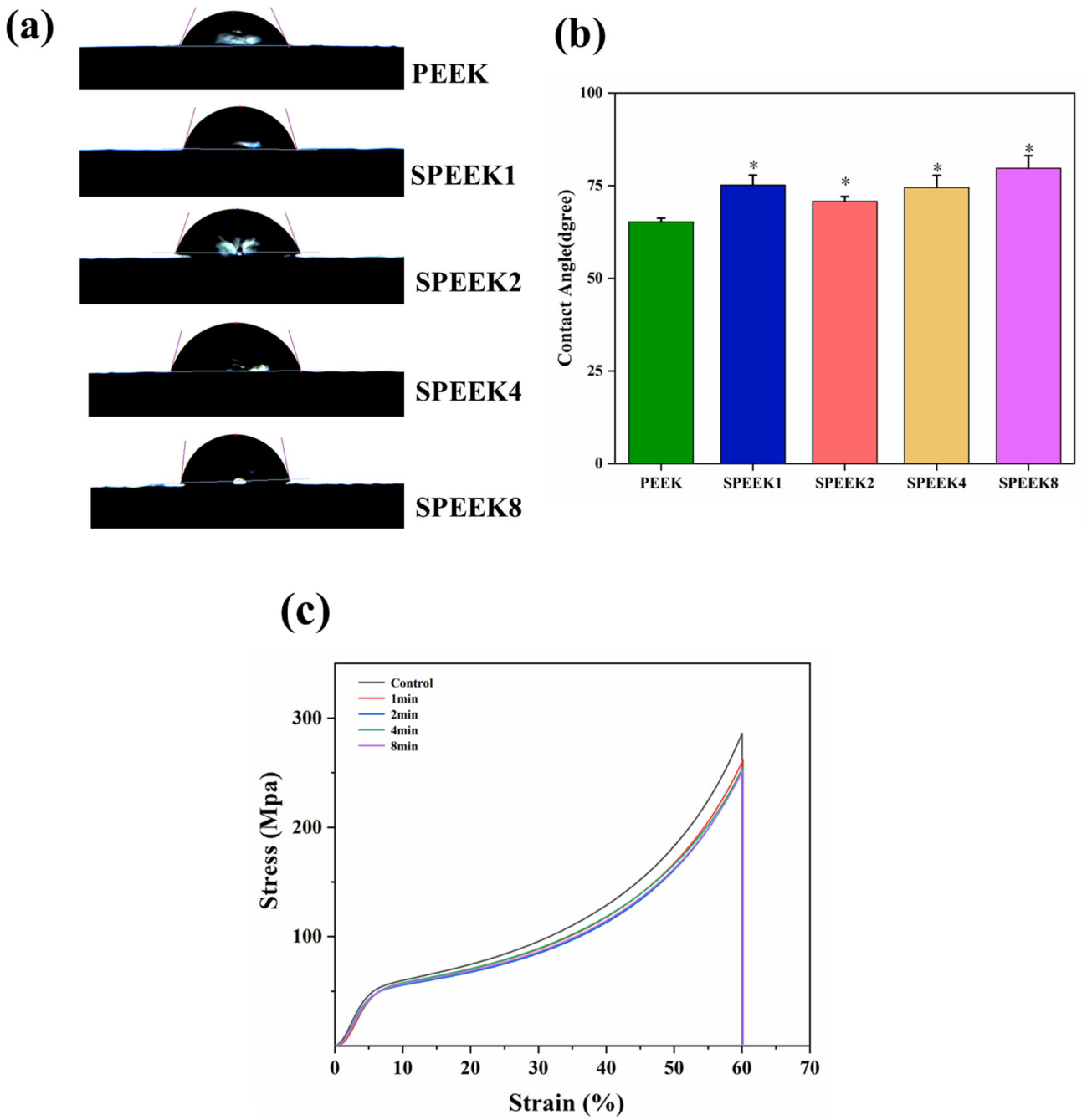

Figure 4. (**a**) Water contact angles of PEEK materials with different sulfonation times. (**b**) Quantitative comparison of water contact angles between different groups. (**c**) The stress–strain curves were obtained by compression tests before and after surface modification of the 3D-printed PEEK phalanx (n = 3, * $p < 0.05$ vs. PEEK control group).

3.3. The Compression Strength of SPEEKs

The compression test showed that when each group of materials was compressed, the samples underwent elastic deformation at the beginning. When the pressure exceeded a certain value, the materials underwent plastic deformation and entered a stable plastic-deformation stage. The pressure continued to increase until the maximum compressive capacity of the samples was reached, and the samples were fractured. No abnormal turning points were observed in the compression curves of all samples, indicating that there were no obvious defects caused by processing or postprocessing. Before sulfonation,

the compression strength of PEEK was (285.74 ± 3.75 MPa, and the compression strength of SPEEKs was (261.57 ± 4.26) MPa, (252.75 ± 5.11) MPa, (254.14 ± 4.79) MPa, and (251.74 ± 3.89) MPa, respectively (Figure 4c). The compressive strength of the sulfonated materials decreased, but there was no significant difference. The results showed that concentrated sulfuric acid treatment did not cause a significant reduction in the compression properties of PEEK.

3.4. The Biological Activity and Biocompatibility of SPEEK Implants

3.4.1. Cell Adhesion and Proliferation

The adhesion of the SHED to the implants is illustrated in Figure 5a. After staining the nuclei of viable cells with DAPI, cell adhesion over the surface of PEEK samples was observed by fluorescence microscopy on day 7. More SHED adhered to the surfaces of PEEK samples after sulfonation treatment than to the surface of the control group, and the number of adherent cells to the surface of SPEEK2 was the highest.

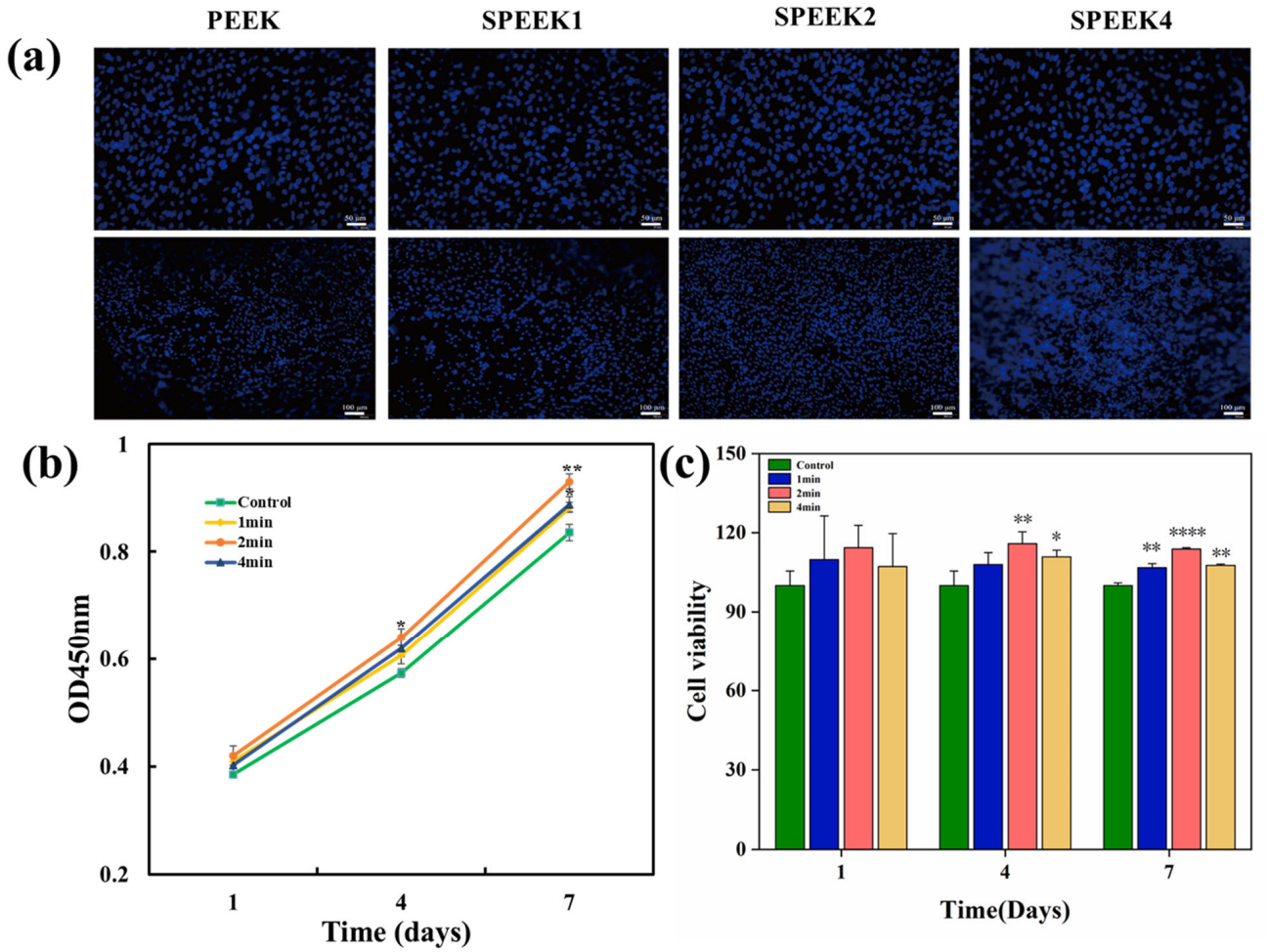

Figure 5. (**a**) Cells stained with DAPI adhered to the surfaces of PEEK. (**b**) Cell growth of pure PEEK and SPEEK at days 1, 4, and 7. Upper scalebar: 50 μm; lower scalebar: 100 μm. (**c**) Cell viability of SHED on surfaces of SPEEKs with different sulfonation times on days 1, 4, and 7 (n = 3, * $p < 0.05$, ** $p < 0.01$, and **** $p < 0.0001$ vs. control group).

Cell proliferation was determined by CCK-8 assays, as shown in Figure 5b. Compared with the control group at days 4 and 7, the SPEEK group showed significantly higher cell proliferation. On day 4, SPEEK2 exhibited more proliferating cells than SPEEK1 and SPEEK4, and there was no significant difference between SPEEK1 and SPEEK4. On days 1, 4, and 7, the cell viability was measured as shown in Figure 5c. On day 1, the cell viability of

the SPEEK group was increased to a certain extent, but there was no significant difference in cell number between the SPEEK group and PEEK control group. On days 4 and 7, the number of cells in the SPEEK group was significantly higher than that of the control group. These results indicated that the sulfonation treatment improved the biocompatibility of the PEEK implants.

3.4.2. Cell Morphology

The SEM micrographs of PEEK surfaces before and after modification show the cell adhesion (Figure 6). SHED can be observed to have a healthy fusiform shape in different cell extensions. The cells on the surface of PEEK were short and spindle-shaped and small in size. Colony formation was observed on the surface of SPEEK2. The cells of colony growth were tightly arranged, and the surrounding cells were short and spindle-shaped [31]. Although the morphology of cells growing on the surface of PEEK implants before and after sulfonation treatment was similar, the adherent cells on the surface of SPEEK2 were the most numerous and closely packed, since a large number of cells were observed under SEM, and a cell-colony formation was observed on the surface of SPEEK2 and not in the other groups.

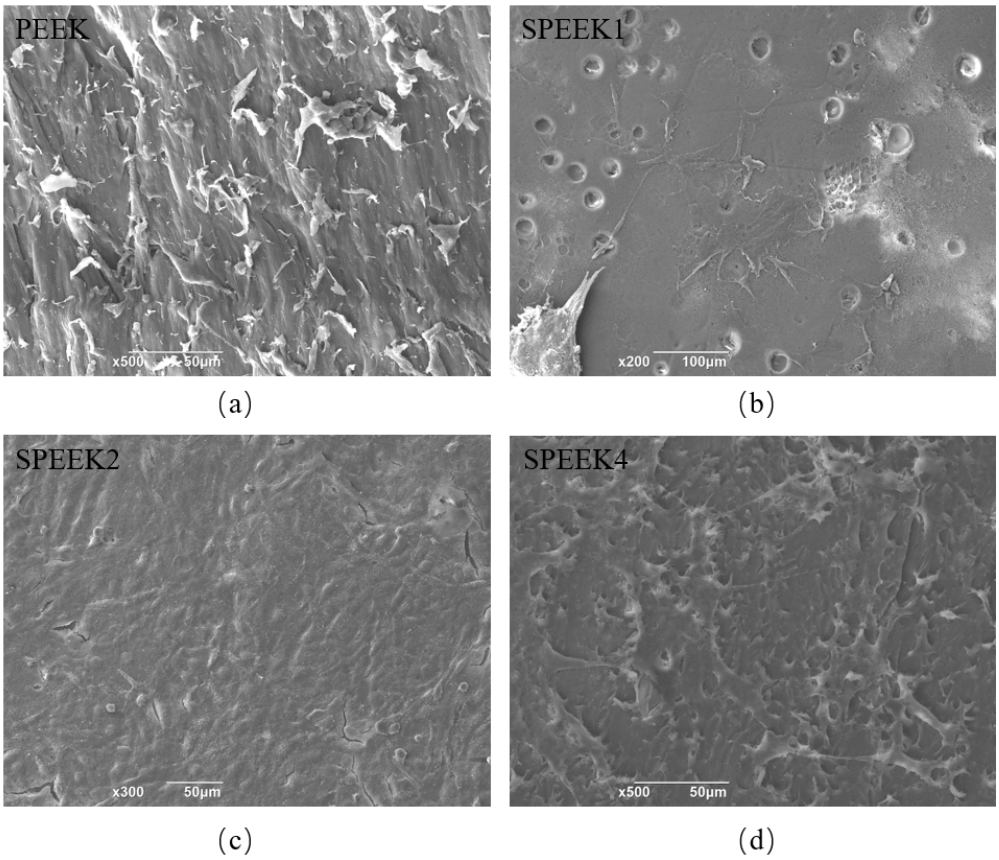

Figure 6. SEM micrographs of adherent cells on PEEK surfaces with sulfonation treatment of (**a**) 0 min (PEEK), (**b**) 1 min (SPEEK1), (**c**) 2 min (SPEEK2), and (**d**) 4 min (SPEEK4), respectively.

3.5. The Osteogenic Ability of SPEEK Implants

3.5.1. ALP Activity

According to the ALP staining (Figure 7a) and its quantitative analysis (Figure 7b), the ALP activity of the SPEEK control group was higher than that of the PEEK group. The results showed that the ALP expression levels of SPEEK were increased on day 7, but there was no significant difference. On day 14, the ALP expression was the highest in the SPEEK2

group and the lowest in the PEEK group, while there was no significant difference between SPEEK1 and SPEEK4.

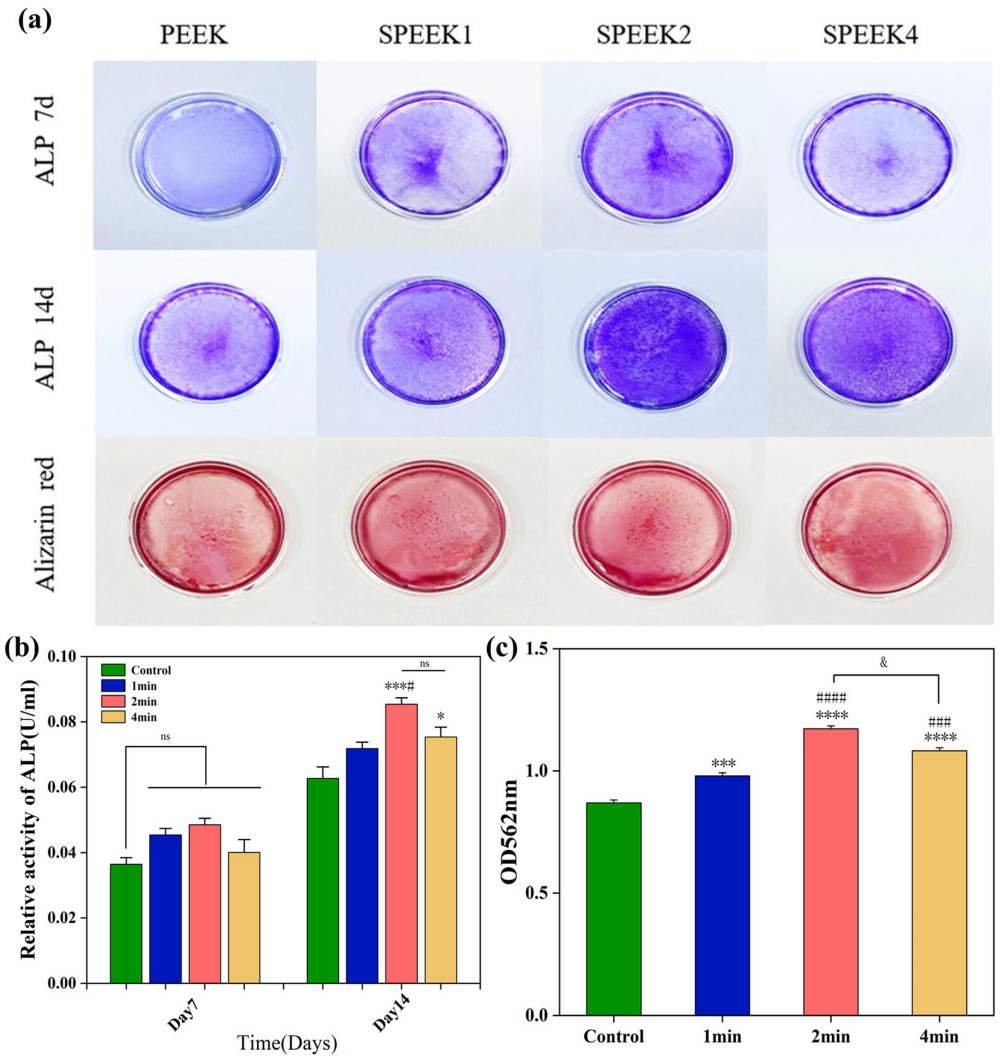

Figure 7. (**a**) ALP staining at 7 and 14 days and alizarin red staining at 21 days in the extracts of pure PEEK and SPEEK index finger. (**b**) Statistical analysis of ALP activity on days 7 and 14. (**c**) Semi-quantitative analysis of Alizarin red staining (n = 3, * $p < 0.05$, *** $p < 0.001$, **** $p < 0.0001$ vs. control group, $^{\#}$ $p < 0.05$, $^{\#\#\#}$ $p < 0.001$, $^{\#\#\#\#}$ $p < 0.0001$ vs. group SPEEK1, and $^{\&}$ $p < 0.05$ group SPEEK2 vs. group SPEEK4).

3.5.2. Extracellular Matrix Mineralization

Alizarin red staining was performed by culturing SHED cells on PEEK material for 21 days to observe the formation of calcium nodules (Figure 7a). The results of ARS showed that only a small amount of red staining was observed in the PEEK control group, and less calcium nodules were formed. Quantitative analysis of ARS (Figure 7c) showed that the degree of nodule mineralization in the SPEEK group was higher than that in the PEEK group, especially in the SPEEK2 group, indicating that the sulfonation can promote cell the extracellular matrix mineralization of PEEK. The results show that SPEEK treated by sulfonation can improve the calcium deposition and osteogenic ability of PEEK implants.

4. Discussion

With the progress of science and medical technology, the new direction of artificial design of prosthesis based on CT data combined with 3D-printing technology for the personalized reconstruction of damaged finger joints is gradually being carried out [32].

As a promising biomaterial, PEEK has been widely used in the biomedical field. Compared with traditional metal implant materials, PEEK has good biocompatibility, and its elastic modulus is close to that of human cortical bone, which can effectively avoid the "stress shielding effect" after implantation. In addition, PEEK also has X-ray penetrability, which can effectively evaluate the postoperative recovery of patients. However, PEEK is biologically inert, which hinders the osseointegration between biomaterials and bone. At the same time, its relatively hydrophobic surface limits cell adhesion and proliferation, leading to poor osseointegration after implantation. Although many methods are currently being developed to improve the bioactivity and osseointegration of PEEK, they still have some limitations for practical orthopedic applications.

To expand PEEK's application, researchers combined it with other bone-growth factors to make inks for 3D-printed prostheses. At present, PEEK has been widely used in skull, jaw, lumbar spine, joint prosthesis, and oral-defect repair. Honigmann et al. used a 3D-printed PEEK scaphoid prosthesis for the first time in clinical practice, confirmed the possibility of 3D-printed PEEK scaphoid prosthesis implantation, and further studied the biomechanical properties of a post-processed PEEK scaphoid prosthesis [33]. Chen et al. introduced the application of a 3D-printed personalized PEEK prosthesis in the reconstruction after a subtotal resection of chronic clavicular osteomyelitis. After two years, the implant did not fail or loosen, and the patient was satisfied with the appearance and shoulder function [34]. Kang et al. used FDM manufacturing technology to manufacture custom-designed rib prostheses and found that its mechanical properties were close to those of natural ribs, and they were successfully implanted and achieved good clinical results [35]. Alipour et al. successfully synthesized injectable aldehyde cellulose nanocrast/fibroin (ADCNCs/SF) hydrogels containing PEEK and affirmed that the hydrogels have good bone inducing ability, making them useful for craniofacial region repair and dental implants [36].

Biomaterials with appropriate 3D nanoporous network surfaces can enhance biological functions in tissue engineering. Immersing PEEK into concentrated sulfuric acid solution can cause sulfonation between PEEK molecules and sulfuric acid, resulting in the generation of charged sulfonic acid groups on the PEEK molecular chain, thereby forming a large number of microscopic pores on the surface to improve its biological activity [37,38]. However, excessive sulfonation not only leads to sulfuric acid residue, but also causes the etching of PEEK at the interface between pores and pores, resulting in the collapse of the pore network, affecting the cytocompatibility of SPEEK, and even leading to the death of cells. Therefore, optimizing the sulfonation time can effectively improve the biological activity of PEEK and reduce the adverse effects on cell compatibility. In this study, PEEK was sulfonated for different times (1 min, 2 min, 4 min, and 8 min). The effects of sulfonation on the surface morphology, chemical composition, hydrophilicity, and compression performance of PEEK were investigated and compared. In addition, the biological properties of SPEEK were further investigated by in vitro experiments.

A 3D micro-nanoporous network was formed on the surface of the sulfonated SPEEK, and the sulfonic acid group was introduced on the surface. We found that the porous structure on the surface of the distal phalanx of SPEEK index finger gradually became more pronounced and complex with increasing sulfonation time. A previous study reported that the formation of nanoporous structures on the SPEEK surface was better with increasing immersion time, which is consistent with our findings [39]. In addition, the microporous structure of SPEEK8 showed excessive dissolution, which also agrees with the results of the measured roughness. In another study [17], it was also found that the microporous structure on the surface of the material showed a tendency to dissolve and destroy when the sulfonation time reached 7 min. This was possibly caused by the excessive degree of sulfonation and protonation of PEEK molecules.

The water contact angle of a biological material is an important indicator of its hydrophilicity and hydrophobicity. Previous studies have shown that changes in surface morphology and the introduction of sulfonic acid groups could affect the surface hydrophilicity of materials to varying degrees [40]. In this study, the water contact angles of

SPEEK groups were larger than those of PEEK, showing that the surface hydrophilicity decreased after sulfonation. This is consistent with previous findings that sulfonated SPEEK has a higher water contact angle than PEEK [41]. The nanotopography and hydrophilicity of the surface are beneficial to the bioactivity and osseointegration of the implant interface. According to previous studies [42], although the hydrophilicity of PEEK surface is reduced under sulfonation, the generated microporous structure is still conducive to improving biological activity. In addition, the compression test of SPEEK showed that its compression properties were not changed after sulfonation treatment, as was consistent with the previous study that found that sulfonation did not change the compression performance of PEEK [43].

The initial interaction of cells with the implant surface is critical for clinical success. In our study, the initial adhesion and proliferation ability of the SPEEK group was better than that of the PEEK group, with SPEEK2 being the best. At the same time, the cell viability of SPEEK group was increased compared with that of the PEEK group. Although the hydrophilicity of SPEEK1 and SPEEK4 decreased after sulfonation treatment, the porous structure of their surfaces increased the specific surface area and roughness of the SPEEK surface. Porous surfaces provide more adsorption sites for cells and proteins, which further promote adhesion and proliferation.

Osteogenic differentiation is essential for the application of bone-repair substitutes. Implants with osteogenic differentiation properties can promote better bone healing. ALP staining and activity assays showed that the non-biologically active nature of the PEEK group resulted in significantly lower ALP activity. In contrast, the extracts of the SPEEK group showed higher ALP activity, in which SPEEK2 reached the highest, indicating that sulfonation treatment was able to promote the osteogenic differentiation of cells, as was consistent with previous studies [44]. Alizarin red staining and semi-quantitative analysis also showed that the osteogenic differentiation ability of SPEEK2 group was better than that of the PEEK group, SPEEK1 group, and SPEEK4 group. Therefore, our results suggest that the sulfonation of PEEK is able to promote the early differentiation of SHED.

From all of these observations, it was found that SPEEK2 has not only a good porous network structure and hydrophilicity, but also has good cell compatibility, proliferation, and differentiation abilities. Wang et al. [18] studied the sulfonation treatment at different reaction times (5 s, 10 s, 30 s, 60 s, and 90 s) by evaluating the hydrophilicity and morphology of the modified PEEK surface; the best sulfonation time was 30 s. The conclusion of Wang's study mainly emphasized the importance of hydrophilicity; it did not consider cytocompatibility, since the sulfonation time was too short. In another study [45], sulfation was performed by immersing PEEK in sulfuric acid for different amounts of time (3 min, 10 min, 30 min, 60 min, and 120 min) at room temperature. Excessive dissolution of the porous material is due to the longer sulfonation time. The authors considered a sulfonation time of 3 min to be the appropriate time for sulfonation. However, their time-point design is crude, and a more appropriate sulfonation time may be 1 to 5 min. Therefore, 2 min was determined as the best sulfonation time for the purposes of characterization, hydrophilicity, biocompatibility, and osteogenic potentials in our study.

5. Conclusions

In conclusion, we used sulfonation treatment to establish a microporous structure on the surface of FDM-fabricated PEEK distal phalanx. Our results show the sulfonation treatment offers a promising way to improve the surface bioactivity of FDM-prepared PEEK implants. Through different times of sulfonation treatment, microporous structures were established on the implant surface, and the surface roughness of the material was improved. Further biological experiments showed that the sulfonation treatment not only promoted the adhesion, proliferation, and bone-specific differentiation of SHED cells on the surface of PEEK implants; it also improved their biological activity. Moreover, when the sulfonation time was 2 min, uniform micropores were formed on the surface of PEEK with an average diameter of (0.71 ± 0.11) μm, which showed little effect on the mechanical

properties of the phalanx and significantly improved SHED cell adhesion, proliferation, and bone-specific differentiation compared with untreated PEEK. Therefore, the optimum sulfonation reaction time for the FDM-printed PEEK phalanx surface was 2 min. Our study provides an idea for the development of PEEK in orthopedics.

Author Contributions: Conceptualization, Y.S. and C.C.; methodology, Y.S.; software, F.Z.; validation, M.R., and L.C.; formal analysis, Y.P. (Yu Peng), Z.Q., L.C. and J.L.; investigation, Z.Q.; resources, T.D., F.Z. and L.C.; data curation, T.D. and Y.P. (Yang Pan); writing—original draft preparation, Y.S.; writing—review and editing, L.C.; visualization, M.R.; supervision, M.R. and L.C.; project administration, L.C. and J.L.; funding acquisition, L.C. and J.L. All authors have read and agreed to the published version of the manuscript.

Funding: This work was supported by Natural Science Foundation of Sichuan Province, China (2022NSFSC1510); Medical Scientific Research Project of Chengdu City, China (2021043); Open Fund Project of Qiang-Yi Medicinal Resources Protection and Utilization Technology Engineering Laboratory, Sichuan Province, China (MZYY202203); the Industry-University Cooperative Education Program of Ministry of Education, China (220506007260254); Higher Education Talent Training Quality and Teaching Reform Project of the Education Department of Sichuan Province, China (JG2021-1102); and the National College Student Innovation and Entrepreneurship Training Program of China (202211079008 and 202211079009).

Institutional Review Board Statement: Not applicable.

Informed Consent Statement: Not applicable.

Data Availability Statement: Not applicable.

Conflicts of Interest: The authors declare no conflict of interest.

References

1. Tuzun, H.Y.; Turkkan, S.; Arsenishvili, A.; Kurklu, M. A new technique for metacarpophalangeal joint replantation after four-finger amputation. *Hand Surg. Rehabil.* **2020**, *39*, 235–237. [CrossRef] [PubMed]
2. Stratton-Powell, A.A.; Pasko, K.M.; Brockett, C.L.; Tipper, J.L. The Biologic Response to Polyetheretherketone (PEEK) Wear Particles in Total Joint Replacement: A Systematic Review. *Clin. Orthop. Relat. Res.* **2016**, *474*, 2394–2404. [CrossRef]
3. Zhao, Y.; Wong, H.M.; Wang, W.; Li, P.; Xu, Z.; Chong, E.Y.; Yan, C.H.; Yeung, K.W.; Chu, P.K. Cytocompatibility, osseointegration, and bioactivity of three-dimensional porous and nanostructured network on polyetheretherketone. *Biomaterials* **2013**, *34*, 9264–9277. [CrossRef]
4. Papathanasiou, I.; Kamposiora, P.; Papavasiliou, G.; Ferrari, M. The use of PEEK in digital prosthodontics: A narrative review. *BMC Oral Health* **2020**, *20*, 217. [CrossRef] [PubMed]
5. Kang, J.; Zhang, J.; Zheng, J.; Wang, L.; Li, D.; Liu, S. 3D-printed PEEK implant for mandibular defects repair—A new method. *J. Mech. Behav. Biomed. Mater.* **2021**, *116*, 104335. [CrossRef] [PubMed]
6. Oladapo, B.I.; Zahedi, S.A.; Ismail, S.O.; Omigbodun, F.T. 3D printing of PEEK and its composite to increase biointerfaces as a biomedical material- A review. *Colloids Surf. B Biointerfaces* **2021**, *203*, 111726. [CrossRef]
7. Basgul, C.; Spece, H.; Sharma, N.; Thieringer, F.M.; Kurtz, S.M. Structure, properties, and bioactivity of 3D printed PAEKs for implant applications: A systematic review. *J. Biomed. Mater. Res. B Appl. Biomater.* **2021**, *109*, 1924–1941. [CrossRef]
8. Theivendran, K.; Arshad, F.; Hanif, U.K.; Reito, A.; Griffin, X.; Foote, C.J. Carbon fibre reinforced PEEK versus traditional metallic implants for orthopaedic trauma surgery: A systematic review. *J. Clin. Orthop. Trauma* **2021**, *23*, 101674. [CrossRef]
9. Han, X.; Yang, D.; Yang, C.; Spintzyk, S.; Scheideler, L.; Li, P.; Li, D.; Geis-Gerstorfer, J.; Rupp, F. Carbon Fiber Reinforced PEEK Composites Based on 3D-Printing Technology for Orthopedic and Dental Applications. *J. Clin. Med.* **2019**, *8*, 240. [CrossRef]
10. Zhang, Y.; Hao, L.; Savalani, M.M.; Harris, R.A.; Di Silvio, L.; Tanner, K.E. In vitro biocompatibility of hydroxyapatite-reinforced polymeric composites manufactured by selective laser sintering. *J. Biomed. Mater. Res. A* **2009**, *91*, 1018–1027. [CrossRef]
11. Wu, X.; Liu, X.; Wei, J.; Ma, J.; Deng, F.; Wei, S. Nano-TiO2/PEEK bioactive composite as a bone substitute material: In vitro and in vivo studies. *Int. J. Nanomed.* **2012**, *7*, 1215–1225.
12. Chu, L.; Li, R.; Liao, Z.; Yang, Y.; Dai, J.; Zhang, K.; Zhang, F.; Xie, Y.; Wei, J.; Zhao, J.; et al. Highly Effective Bone Fusion Induced by the Interbody Cage Made of Calcium Silicate/Polyetheretherketone in a Goat Model. *ACS Biomater. Sci. Eng.* **2019**, *5*, 2409–2416. [CrossRef]
13. Yu, D.; Lei, X.; Zhu, H. Modification of polyetheretherketone (PEEK) physical features to improve osteointegration. *J. Zhejiang Univ. Sci. B* **2022**, *23*, 189–203. [CrossRef] [PubMed]
14. Lu, T.; Wen, J.; Qian, S.; Cao, H.; Ning, C.; Pan, X.; Jiang, X.; Liu, X.; Chu, P.K. Enhanced osteointegration on tantalum-implanted polyetheretherketone surface with bone-like elastic modulus. *Biomaterials* **2015**, *51*, 173–183. [CrossRef] [PubMed]

15. Bakar, M.A.; Cheng, M.H.; Tang, S.M.; Yu, S.C.; Liao, K.; Tan, C.T.; Khor, K.A.; Cheang, P. Tensile properties, tension-tension fatigue and biological response of polyetheretherketone-hydroxyapatite composites for load-bearing orthopedic implants. *Biomaterials* **2003**, *24*, 2245–2250. [CrossRef] [PubMed]
16. Dos Santos, F.S.F.; Vieira, M.; da Silva, H.N.; Tomás, H.; Fook, M.V.L. Surface Bioactivation of Polyether Ether Ketone (PEEK) by Sulfuric Acid and Piranha Solution: Influence of the Modification Route in Capacity for Inducing Cell Growth. *Biomolecules* **2021**, *11*, 1260. [CrossRef]
17. Ma, R.; Wang, J.; Li, C.; Ma, K.; Wei, J.; Yang, P.; Guo, D.; Wang, K.; Wang, W. Effects of different sulfonation times and post-treatment methods on the characterization and cytocompatibility of sulfonated PEEK. *J. Biomater. Appl.* **2020**, *35*, 342–352. [CrossRef]
18. Wang, W.; Luo, C.J.; Huang, J.; Edirisinghe, M. PEEK surface modification by fast ambient-temperature sulfonation for bone implant applications. *J. R. Soc. Interface* **2019**, *16*, 20180955. [CrossRef]
19. de Sá, M.D.; de Lima Souza, J.W.; da Silva, H.N.; Torres, R.H.; Leite, M.D.; Barbosa, R.C.; Leite, I.F.; Pimentel, C.A.; Fook, M.V. Biocompatible Sulphonated PEEK Spheres: Influence of Processing Conditions on Morphology and Swelling Behavior. *Polymers* **2021**, *13*, 2920. [CrossRef]
20. Boaretti, C.; Roso, M.; Lorenzetti, A.; Modesti, M. Synthesis and Process Optimization of Electrospun PEEK-Sulfonated Nanofibers by Response Surface Methodology. *Materials* **2015**, *8*, 4096–4117. [CrossRef]
21. Sun, Y.; Liu, X.; Tan, J.; Lv, D.; Song, W.; Su, R.; Li, L.; Liu, X.; Ouyang, L.; Liao, Y. Strontium ranelate incorporated 3D porous sulfonated PEEK simulating MC3T3-E1 cell differentiation. *Regen. Biomater.* **2020**, *8*, rbaa043. [CrossRef]
22. Brum, R.S.; Monich, P.R.; Fredel, M.C.; Contri, G.; Ramoa, S.D.A.S.; Magini, R.S.; Benfatti, C.A.M. Polymer coatings based on sulfonated-poly-ether-ether-ketone films for implant dentistry applications. *J. Mater. Sci. Mater. Med.* **2018**, *29*, 132. [CrossRef] [PubMed]
23. Yee, R.S.; Zhang, K.; Ladewig, B.P. The Effects of Sulfonated Poly(ether ether ketone) Ion Exchange Preparation Conditions on Membrane Properties. *Membranes* **2013**, *3*, 182–195. [CrossRef] [PubMed]
24. Yuan, X.; Ouyang, L.; Luo, Y.; Sun, Z.; Yang, C.; Wang, J.; Liu, X.; Zhang, X. Multifunctional sulfonated polyetheretherketone coating with beta-defensin-14 for yielding durable and broad-spectrum antibacterial activity and osseointegration. *Acta Biomater.* **2019**, *86*, 323–337. [CrossRef] [PubMed]
25. Wan, T.; Jiao, Z.; Guo, M.; Wang, Z.; Wan, Y.; Lin, K.; Liu, Q.; Zhang, P. Gaseous sulfur trioxide induced controllable sulfonation promoting biomineralization and osseointegration of polyetheretherketone implants. *Bioact. Mater.* **2020**, *5*, 1004–1017. [CrossRef] [PubMed]
26. Fan, L.; Guan, P.; Xiao, C.; Wen, H.; Wang, Q.; Liu, C.; Luo, Y.; Ma, L.; Tan, G.; Yu, P.; et al. Exosome-functionalized polyetheretherketone-based implant with immunomodulatory property for enhancing osseointegration. *Bioact. Mater.* **2021**, *6*, 2754–2766. [CrossRef]
27. Yuan, B.; Cheng, Q.; Zhao, R.; Zhu, X.; Yang, X.; Yang, X.; Zhang, K.; Song, Y.; Zhang, X. Comparison of osteointegration property between PEKK and PEEK: Effects of surface structure and chemistry. *Biomaterials* **2018**, *170*, 116–126. [CrossRef] [PubMed]
28. Kahn, J.S.; Hu, Y.; Willner, I. Stimuli-Responsive DNA-Based Hydrogels: From Basic Principles to Applications. *Acc. Chem. Res.* **2017**, *50*, 680–690. [CrossRef] [PubMed]
29. Yuan, Z.; Long, T.; Zhang, J.; Lyu, Z.; Zhang, W.; Meng, X.; Qi, J.; Wang, Y. 3D printed porous sulfonated polyetheretherketone scaffold for cartilage repair: Potential and limitation. *J. Orthop. Translat.* **2022**, *33*, 90–106. [CrossRef]
30. Zheng, Z.; Liu, P.; Zhang, X.; Xin, J.; Wang, Y.; Zou, X.; Mei, X.; Zhang, S.; Zhang, S. Strategies to improve bioactive and antibacterial properties of polyetheretherketone (PEEK) for use as orthopedic implants. *Mater. Today Bio.* **2022**, *16*, 100402.
31. Subhi, H.; Husein, A.; Mohamad, D.; Nik Abdul Ghani, N.R.; Nurul, A.A. Chitosan-Based Accelerated Portland Cement Promotes Dentinogenic/Osteogenic Differentiation and Mineralization Activity of SHED. *Polymers* **2021**, *13*, 3358. [CrossRef] [PubMed]
32. Nyberg, E.L.; Farris, A.L.; Hung, B.P.; Dias, M.; Garcia, J.R.; Dorafshar, A.H.; Grayson, W.L. 3D-Printing Technologies for Craniofacial Rehabilitation, Reconstruction, and Regeneration. *Ann. Biomed. Eng.* **2017**, *45*, 45–57. [CrossRef]
33. Honigmann, P.; Sharma, N.; Schumacher, R.; Rueegg, J.; Haefeli, M.; Thieringer, F. In-Hospital 3D Printed Scaphoid Prosthesis Using Medical-Grade Polyetheretherketone (PEEK) Biomaterial. *Biomed. Res. Int.* **2021**, *2021*, 1301028. [CrossRef] [PubMed]
34. Chen, C.; Yin, Y.; Xu, H.; Li, Z.; Wang, F.; Chen, G. Personalized three-dimensional printed polyether-ether-ketone prosthesis for reconstruction after subtotal removal of chronic clavicle osteomyelitis: A case report. *Medicine* **2021**, *100*, e25703. [CrossRef] [PubMed]
35. Kang, J.; Wang, L.; Yang, C.; Wang, L.; Yi, C.; He, J.; Li, D. Custom design and biomechanical analysis of 3D-printed PEEK rib prostheses. *Biomech. Model Mechanobiol.* **2018**, *17*, 1083–1092. [CrossRef]
36. Alipour, M.; Ghorbani, M.; Johari khatoonabad, M.; Aghazadeh, M. A novel injectable hydrogel containing polyetherether-ketone for bone regeneration in the craniofacial region. *Sci. Rep.* **2023**, *13*, 864. [CrossRef] [PubMed]
37. Ouyang, L.; Zhao, Y.; Jin, G.; Lu, T.; Li, J.; Qiao, Y.; Ning, C.; Zhang, X.; Chu, P.K.; Liu, X. Influence of sulfur content on bone formation and antibacterial ability of sulfonated PEEK. *Biomaterials* **2016**, *83*, 115–126. [CrossRef]
38. Chen, J.-C.; Chen, C.-H.; Chang, K.-C.; Liu, S.-M.; Ko, C.-L.; Shih, C.-J.; Sun, Y.-S.; Chen, W.-C. Evaluation of the Grafting Efficacy of Active Biomolecules of Phosphatidylcholine and Type I Collagen on Polyether Ether Ketone: In Vitro and In Vivo. *Polymers* **2021**, *13*, 2081. [CrossRef]

39. Su, Y.; He, J.; Jiang, N.; Zhang, H.; Wang, L.; Liu, X.; Li, D.; Yin, Z. Additively-manufactured poly-ether-ether-ketone (PEEK) lattice scaffolds with uniform microporous architectures for enhanced cellular response and soft tissue adhesion. *Mater. Des.* **2020**, *191*, 108671. [CrossRef]
40. Guo, C.; Lu, R.; Wang, X.; Chen, S. Antibacterial activity, bio-compatibility and osteogenic differentiation of graphene oxide coating on 3D-network poly-ether-ether-ketone for orthopaedic implants. *J. Mater. Sci. Mater. Med.* **2021**, *32*, 135. [CrossRef]
41. Zhu, Y.; Cao, Z.; Peng, Y.; Hu, L.; Guney, T.; Tang, B. Facile Surface Modification Method for Synergistically Enhancing the Biocompatibility and Bioactivity of Poly(ether ether ketone) That Induced Osteodifferentiation. *ACS Appl. Mater. Interfaces* **2019**, *11*, 27503–27511. [CrossRef] [PubMed]
42. Chai, H.; Sang, S.; Luo, Y.; He, R.; Yuan, X.; Zhang, X. Icariin-loaded sulfonated polyetheretherketone with osteogenesis promotion and osteoclastogenesis inhibition properties via immunomodulation for advanced osseointegration. *J. Mater. Chem. B* **2022**, *10*, 3531–3540. [CrossRef] [PubMed]
43. Yin, J.; Han, Q.; Zhang, J.; Liu, Y.; Gan, X.; Xie, K.; Xie, L.; Deng, Y. MXene-Based Hydrogels Endow Polyetheretherketone with Effective Osteogenicity and Combined Treatment of Osteosarcoma and Bacterial Infection. *ACS Appl. Mater. Interfaces* **2020**, *12*, 45891–45903. [CrossRef] [PubMed]
44. Wang, C.; Wang, S.; Yang, Y.; Jiang, Z.; Deng, Y.; Song, S.; Yang, W.; Chen, Z.G. Bioinspired, biocompatible and peptide-decorated silk fibroin coatings for enhanced osteogenesis of bioinert implant. *J. Biomater. Sci. Polym. Ed.* **2018**, *29*, 1595–1611. [CrossRef] [PubMed]
45. Cheng, Q.; Yuan, B.; Chen, X.; Yang, X.; Lin, H.; Zhu, X.; Zhang, K.; Zhang, X. Regulation of surface micro/nano structure and composition of polyetheretherketone and their influence on the behavior of MC3T3-E1 pre-osteoblasts. *J. Mater. Chem. B* **2019**, *7*, 5713–5724. [CrossRef]